

1 **A Custom Microcontrolled and Wireless-Operated Chamber** 2 **for Auditory Fear Conditioning**

3
4 **Authors:** Paulo Aparecido Amaral Júnior^{1,2#}, Flávio Afonso Gonçalves Mourão^{1#},
5 Mariana Chamon Ladeira Amâncio¹, Hyorrana Pereira Pinto¹, Vinícius Rezende
6 Carvalho^{1,2}, Leonardo de Oliveira Guarnieri^{1,2}, Hermes Aguiar Magalhães², Márcio
7 Flávio Dutra Moraes^{1*}.

8
9 ¹ Núcleo de Neurociências, Departamento de Fisiologia e Biofísica, Instituto de Ciências
10 Biológicas (ICB), Universidade Federal de Minas Gerais (UFMG). Av. Antônio Carlos,
11 6627 - CEP 31270-901. Belo Horizonte, Minas Gerais, Brazil.

12 ² Programa de Pós-Graduação em Engenharia Elétrica, Departamento de Engenharia
13 Eletrônica (DELT), Escola de Engenharia, Universidade Federal de Minas Gerais
14 (UFMG). Av. Antônio Carlos, 6627 - CEP 31270-901. Belo Horizonte, Minas Gerais,
15 Brazil.

16
17 # These authors have contributed equally to this work.

18 *** Correspondence:**

19 Márcio Flávio Dutra Moraes, PhD
20 Núcleo de Neurociências, Departamento de Fisiologia e Biofísica
21 Instituto de Ciências Biológicas (ICB)
22 Universidade Federal de Minas Gerais (UFMG)
23 Av. Antônio Carlos, 6627 - CEP 31270-901- Campus Pampulha
24 Belo Horizonte - MG - Brazil
25 Fax: +55 31 3409-2924 Phone: +55 31 3409-2939
26 Email: mfdm@ufmg.br

27
28
29
30 **Keywords:** Classical fear conditioning, Custom conditioning chamber, Laboratory
31 equipment, Internet of things, Arduino, ESP8266.

32

33 **ABSTRACT**

34

35 Animal behavioral paradigms, such as classical conditioning and operant conditioning,
36 are an important tool to study the neural basis of cognition and behavior. These paradigms
37 involve manipulating sensory stimuli in a way that learning processes are induced under
38 controlled experimental conditions. However, the majority of the commercially available
39 equipment did not offer flexibility to manipulate stimuli. Therefore, the development of
40 most versatile devices would allow the study of more complex cognitive functions. The
41 purpose of this work is to present a low-cost, customized and wireless-operated chamber
42 for animal behavior conditioning, based on the joint operation of two microcontroller
43 modules: Arduino Due and ESP8266-12E. Our results showed that the auditory
44 stimulation system allows setting the carrier frequency in the range of 1 Hz up to more
45 than 100 kHz and the sound stimulus can be modulated in amplitude, also over a wide
46 range of frequencies. Likewise, foot-shock could be precisely manipulated regarding its
47 amplitude (from ~200 μ A to ~1500 μ A) and frequency (up to 20 pulses per second).
48 Finally, adult rats exposed to a protocol of cued fear conditioning in our device showed
49 consistent behavioral response and electrophysiological evoked responses in the midbrain
50 auditory pathway. Furthermore, the device developed in the current study represents an
51 open source alternative to develop customized protocols to study fear memory under
52 conditions of varied sensory stimuli.

53 **INTRODUCTION**

54

55 Animal behavioral paradigms have long played an important role in understanding
56 the underlying neurobiological mechanisms of learning and memory processes;
57 ubiquitously considered one of the greatest challenges in Neuroscience (Squire, 2009). In
58 Classical or Pavlovian Conditioning, animal innate or reflex responses become evocable
59 by stimuli that are usually neutral (such as sound or visual stimuli), if previously paired
60 with an emotionally relevant stimuli, characterizing the basis of an associative learning
61 process (Kim and Jung, 2006). Using a more appropriate terminology, the conditioned
62 responses (CR) are established under an appropriate contingency of unconditioned
63 stimulus (US) presentations paired with the conditioned stimulus (CS) occurrences
64 (Baron, 1959; Holland, 1977). Proper controls undergo the exact same procedure aside
65 from the fact that CS or US can be presented alone or CS is not paired in time with the
66 US (Rescorla, 1967). Although the laboratory equipments designed to perform such
67 associative learning protocols are supposedly fairly simple, the price can be prohibitive
68 for small budget projects and they are usually quite inflexible in terms of controlling and
69 programming the stimuli. The latter may constitute a drawback for the design of
70 customized behavioral paradigms which may use amplitude modulated stimuli in order
71 to isolate neural circuitry involved in the sensory processing by means of steady state
72 evoked responses (Lockmann et al., 2017; Pinto et al., 2017). In addition, the study of
73 more complex cognitive and behavioral processes becomes impracticable, since they
74 require more sophisticated and robust means of controlling contextual parameters and
75 interacting with the animals (Cushman et al., 2013).

76 Fortunately, custom development of laboratory tools is becoming more feasible
77 with the advances in technology (Buccino et al., 2018; Pineño, 2014; Siegle et al., 2017;
78 Sinard and Gershkovich, 2012; White et al., 2019). Mainly, low-cost commercially
79 available microcontroller modules have recently achieved a high level of integration and
80 processing power, encouraging their acquisition and use in research laboratories.
81 Arduino, for example, is an attractive hardware and software open-source solution
82 (D'Ausilio, 2012) to program several different families of microcontrollers for a number
83 of different consumer needs (Pineño, 2014; Teikari et al., 2012).

84 Considering this scenario, the purpose of our work is to present a customized,
85 low-cost, microcontrolled and wireless-operated device for animal behavior conditioning.
86 We propose a scalable architecture, based on Arduino Due board and ESP8266-12E
87 module, which allows adding different sensory stimuli and behavioral feedback aside
88 from what we chose to depict in this work (i.e. programmable sound stimulation waves
89 and electric shock). Likewise, other elements, such as sensors, actuators and
90 touchscreens, can be easily integrated to the apparatus by connecting them to innumerable
91 general-purpose input/output (GPIO) pins available, or through digital communication
92 protocols, like I2C, UART or SPI. This allows the design of a low-cost widely equipped
93 apparatus and eases the development of customized behavioral paradigms.

94

95

96 **METHOD**

97

98 **SYSTEM OVERVIEW**

99

100 The main electronic components of the custom conditioning chamber are the
101 ESP8266-12E module (<https://www.adafruit.com/product/2491>) and the Arduino Due
102 board (<https://store.arduino.cc/usa/due>). The first one is an internet-of-things device from

103 Espressif company, available since 2014. It has a Tensilica L106 32-bit microcontroller
104 and an 80 MHz CPU clock. It operates at 3.3 V and supports WiFi (IEEE 802.11 g/b/n),
105 I2C, SPI and UART communication protocols. Eleven GPIO pins and 32 kB RAM are
106 available in the module. The ESP8266 is used here mainly as a programmable and flexible
107 user interface, presented on a web page format, to allows users to write and read
108 parameters to the device without the need of physically implementing buttons, knobs and
109 displays.

110 The Arduino Due is a 32-bit microcontroller board based on the Atmel SAM3X8E
111 ARM Cortex-M3 CPU. It has a 84 MHz CPU clock, 54 digital input/output pins, 12
112 analog inputs, 2 DAC (digital to analog) and can communicate through SPI, I2C, UART
113 and USB.

114 Both modules are programmed with an Arduino sketch (*Web_Page.ino* for the
115 ESP8266-12E and *Stimuli.ino* for the Arduino Due) with specific assignments and they
116 cooperate to produce all the apparatus functionality. The modules communicate with each
117 other via a 16-bit serial peripheral interface (SPI) and through digital signaling via two
118 GPIO pins. In the scope of this work, systems for auditory and electrical stimulation
119 (footshock) were implemented, stimuli that can be used as CS and US, respectively, in
120 behavioral paradigms (Figure 1).

121 The auditory stimulating system consists of a 12-bit digital-to-analog converter
122 (DAC; available at Arduino Due board), a commercial audio amplifier and a speaker. The
123 footshock system, in turn, is formed by a high DC-voltage ($310 V_{DC}$) supply circuit in
124 series with a current limiting resistor, significantly higher than the animal's resistance, in
125 series with a variable resistor in order to deliver a short pulse of constant current through
126 the bars on the chamber. The footshock system was designed to limit stimulus intensity
127 between $\sim 200 \mu A$ and $\sim 1500 \mu A$ and can be manually set by a potentiometer and an
128 ammeter. Embedded electronics were designed to have only one bar under the animal, at
129 a specific time, serving as current sink. The rate that bars are "scanned" and the duration
130 of each shock pulse are programmable. The user interface for operating the apparatus was
131 developed in a web interface, implemented in HTML within the *Web_Page.ino* sketch,
132 making it not only very flexible and comprehensive in terms of controlling system
133 parameters. Parameters such as sound and shock onset (seconds), shock pulses intervals
134 between bars (milliseconds to seconds), sound intensity (%), sound carrier frequency (Hz)
135 and modulating frequency (Hz) can be remotely programmed to perform the experiments.
136 In addition, each added trial can be saved by simply insert the parameters into a sequence
137 and loaded it in later experimental sessions (Figure 2). Thus, behavioral paradigms can
138 be easily configured using iPads, smartphones, notebooks or any device with a Wi-Fi
139 connection.

140

141 *Hardware Design*

142

143 The custom conditioning chamber dimensions are $330 \times 200 \times 300 \text{ mm}^3$ (length,
144 width and height, respectively), built with 5 mm-thick transparent acrylic boards. An
145 acrylic board covers the chamber, preventing the animals from escaping the context
146 (Figure 3A-C). The chamber floor is built with 16 stainless steel cylindrical bars, 250
147 mm-long and 5 mm in diameter each. They are arranged in parallel, spaced 20 mm from
148 each other and placed through small bilateral holes with 0.6 cm in diameter. The number
149 of bars can be increased up to 32 and spaced 7.5 mm from each other.

150

151 In order to deliver the shock through the bars, a $127 V_{AC} : 220 V_{AC}$ transformer
152 (0.03 kVA) raises and isolates the AC voltage from the electric grid. A diode rectifier
bridge (2KBP06M; 600 V / 2A) and electrolytic capacitor ($10 \mu F / 350 V$) at the rectifier

153 output produce a constant voltage of approximately $310 V_{DC}$. The high voltage end passes
154 through a current limiting resistor, set to a maximum of 1-2 mA, and then through a
155 variable resistor in order to "fine tune" the output current. The current remains fairly
156 stable since both resistors are within an order of magnitude higher than the conductance
157 changes expected from the animal stepping on the bars and closing the circuit. Finally, a
158 series of simple common-emitter circuits, using bipolar transistors (BC547B) as switches
159 are used to drive optocouplers (PC817) in order to deliver a current pulse to each
160 individual bar, therefore guaranteeing that whatever combination of bars the animal is
161 stepping on will still deliver the foot shock. The bars are sequentially "scanned" at a
162 programmable interval and the pulse duration can also be set by the user. The Arduino
163 Due board outputs a set of digital signals that control each bar potential. Altogether, this
164 constitutes an aversive stimulating system for US presentations (Figure 3E).

165 A 12-bit digital-to-analog converter at Arduino Due is used to generate analog
166 waveform. The algorithm behind signal generation is the following: 1) a set of 8 points
167 (2 bytes each) form the template of a sinusoidal waveform - or any period of a
168 programmable signal - that will be repeated at the carrier frequency. Thus, the sampling
169 frequency (f_a) of the D/A output will be 8 times that of the carrier frequency (f_c). 2) The
170 amplitude of each 8 sample block will be proportionally given by each byte of a sequence
171 of bytes representing the modulation frequency (f_m). That is, the sequence of bytes is
172 composed by a minimum of $f_a/(f_m \cdot 8)$ bytes repeated up to the duration set by the user.
173 In this way, we were able to generate quite a variety of stimulation waveforms at a very
174 low computational cost (within the range of allowing ultrasound stimulation) and using
175 few parameters and/or memory (Figure 4A-D).

176 177 *Firmware Design*

178
179 Arduino software applications were implemented for operating and controlling
180 the custom chamber: *Web_Page.ino*, uploaded to ESP8266-12E module, and *Stimuli.ino*,
181 uploaded to Arduino Due board.

182 Programmed with *Web_Page.ino* sketch, ESP8266-12E module takes care of
183 basically two things: (1) it provides the user interface, through which the experimental
184 protocols can be programmed (this interface is a web page, available from an independent
185 access point WiFi network managed by the ESP8266-12E), and; (2) it uses 2 GPIO pins
186 to determine when the Arduino Due should turn the conditioned (CS) and unconditioned
187 (US) stimuli on or off, according to the parameters specified via web interface (Figure
188 2).

189 Programmed with *Stimuli.ino* sketch, Arduino Due board takes care of generating
190 CS and US with specific temporal patterns, as specified by user. This routine manages
191 triggers and CPU interruptions in order to generate, at the Arduino DAC output, an analog
192 waveform with carrier and modulating frequencies, as well as a specific amplitude. In
193 addition, GPIO pins are used to control each bar potential to produce custom aversive
194 footshock patterns.

195 196 SYSTEM VALIDATION

197
198 The validation of the customized apparatus was made in two steps. At first, bench
199 tests were carried out in order to verify the correct functionality of the circuits, safety
200 specifications and firmware for CS and US presentation before using the system in a
201 living organism. In the second stage, experimental animals were submitted to a classical
202 fear conditioning (CFC) task using Auditory Steady State Stimulation (ASSR - 10 kHz

203 carrier frequency modulated at 53.7 Hz) while recording local field potentials in the
204 Inferior Colliculus (IC), the principal midbrain nucleus of the auditory pathway. The IC
205 recordings show stable oscillations at the same frequency of the stimulus amplitude
206 modulating component (i.e. when stimuli are turned-on), reflecting entrainment of
207 neurons responding to sound. This particular steady-state evoked potential (SSEP) neural
208 response is called an ASSR (Kuwada et al., 1986; Picton et al., 2003).

209

210 *Bench tests*

211

212 In order to assess the flexibility in programming the sound stimulus, as well as the
213 precision of its configurable parameters (mainly carrier frequency and modulating
214 frequency), different sound stimuli reproduced by the audio system were recorded by
215 means of a microphone and placed inside the customized chamber. The sampling
216 frequency employed was 96 kHz and the raw data were qualitatively analyzed with
217 custom-made and built-in MATLAB codes (MATLAB R2016a). The time-frequency
218 power of the carrier and modulating frequency were calculated by the standard built-in
219 spectrogram function (short-time Fourier transform-STFT; non overlapping, 2,048-point
220 Hamming window). In the case of the modulating frequency, the audio signals were
221 preprocessed so that only the envelope of the signal (thus, the modulating signal) was
222 considered. This was accomplished by means of the built-in Matlab Hilbert transform
223 function.

224

225 In order to determine the flexibility and precision of the aversive electrical
226 stimulus, a 20 k Ω resistor was connected between two bars of the chamber, simulating
227 the resistance of a rodent that could eventually be touching them (Figure 6A). Similar
228 values of resistance for rats were reported in previous work (Walters and Tullis, 1966).
229 The voltage drop across this resistor was measured with an oscilloscope (GDS-2202A
230 GW INSTEK) for four different programmed shock values (400 μ A, 600 μ A, 800 μ A and
231 1000 μ A) during one second time course (Figure 6B), so that the electric current could be
232 easily determined using Ohm's Law.

232

233 Additionally, another bench test evaluated how much the footshock intensity
234 changes with respect to variability in animal body conductance (which can occur due to
235 humidity and different body masses between animals). For this, a 400 μ A footshock was
236 programmed and its intensity was measured in three different cases: R = 15 k Ω , R = 20
237 k Ω and R = 25 k Ω (Figure 6D-E).

237

238 *Proof of concept: Classical fear conditioning (CFC) and Local field potential (LFP)* 239 *recordings*

240

241 Male *Rattus norvegicus* (Wistar) weighing 270-310 g were supplied by the
242 *Instituto de Ciências Biológicas 2* (BICBIO 2) vivarium, housed under controlled
243 environmental conditions (22 ± 2 °C), with a 12:12 h light-dark cycle and free access to
244 food and water. All experiments were approved by the Institutional Animal Care and Use
245 Committee at the *Universidade Federal de Minas Gerais* (CEUA-UFMG; protocol no.
246 112/2014.), and were conducted in accordance with *Conselho Nacional de Controle de*
247 *Experimentação Animal* (CONCEA) guidelines defined by Arouca Act 11.794 under
248 Brazilian federal law. CEUA directives comply with National Institutes of Health (NIH)
249 guidelines for the care and use of animals in research.

250

251

252

253 *Surgery*

254

255 Animals were anesthetized intraperitoneally with ketamine/xylazine solution (15
256 mg/kg and 80 mg/kg, respectively), the head surface was shaved and then the animal was
257 positioned in a stereotaxic frame (Stoelting, Wood Dale, IL). After asepsis with alcohol
258 (70%, topical) and povidineiodine solution (7.5%, topical) a local anesthesia with
259 lidocaine clorohydrate-epinephrine [1% (wt/vol), 7 mg/kg] was applied and an incision
260 in the scalp was made to expose the skull.

261 Monopolar electrodes for recording, made of a twisted pair of stainless-steel
262 (0.005 in.) teflon-coated wires (Model 791400, A-M Systems Inc., Carlsborg, WA, USA)
263 was slowly lowered and positioned at the ventral region of the left IC central nucleus (AP:
264 -9.0 mm referenced from the bregma, ML: -1.4 mm, DV: -4.0 mm) (Paxinos and Watson
265 2007). The coordinates for electrode positioning were chosen according to the tonotopic
266 organization of the IC since the ventral layers respond better to the high frequencies
267 (Clopton and Winfield, 1973; Malmierca et al., 2008) as used in the CFC protocol. At the
268 end stainless steel screws were implanted on the nasal bones (anterior to the olfactory
269 bulb), one to the left as the reference electrode (0 V) and another one as the ground. Both
270 reference/ground and recording electrodes were soldered in a RJ-11 connector, which was
271 fixed to the skull with dental acrylic. Animals received a prophylactic treatment with
272 pentantibiotics (Zoetis Fort Dodge; 19 mg/kg) and anti-inflammatory (Banamine, 2.5
273 mg/kg) to prevent discomfort and infection after surgery and recovery for 7 day.

274

275 *Classical fear conditioning (CFC).*

276

277 The CS used in the CFC was a 10 kHz pure tone with its amplitude modulated by
278 a sine wave of 53.7 Hz. These specific tone features were chosen based on previous results
279 (Lockmann et al., 2017; Pinto et al., 2017).

280 The amplitude modulated tone generated by the customized conditioning chamber
281 was amplified by a commercial sound amplifier (AB100, 100 WRMS, 4 Ω , NCA) and
282 reproduced by a speaker (ST304, 40 WRMS, 8 Ω , Selenium Super Tweeter).

283 Before the behavioral sessions, the intensity of the CS tone was measured and set
284 to 85 dB SPL at the center of the conditioning chamber (Brüel & Kjær type 2238 sound
285 level meter). This sound pressure level ensures an appropriate electrophysiological
286 response considering the anatomical positioning of the recording electrode (Malmierca et
287 al., 2008; Meeren et al., 2001).

288 CFC was performed on three consecutive days in two different contexts (Figure
289 3A). On the first day (preconditioning), ten rats were presented with 5 CS stimuli (30 s
290 each apart from each other, with pseudorandom interval not longer than 120 seconds) in
291 the context A (a black acrylic box, 30 x 20 x 25 cm³ with one transparent face and 10%
292 alcohol solution scented).

293 On the second day (conditioning), the behavioral task took place in the context B,
294 which is the custom chamber proposed in this work (with 0.001% acetic Acid solution
295 scented). The rats were randomly assigned to paired (n = 5) or unpaired (n = 5) groups
296 and similarly to the day 1, five CS stimuli were presented, however five US were applied.
297 The US consisted of a 400 μ A current applied through metal bars on the floor over 2 s
298 (Mourão et al., 2016). In the paired group, each presentation of CS was temporally paired
299 with US in the last two seconds of the CS presentations. On the other hand, in the unpaired
300 group, US occurred at random times between CS.

301 On the third day (retention test), rats were presented to an accurate repetition of
302 the preconditioning procedure. Returning to the context A (10% alcohol solution scented),

303 all animals were presented with 5 CS stimuli (30 s apart from each other, with
304 pseudorandom interval not longer than 120 seconds).

305 The sessions were recorded by a camera set up in front of the box, and the videos
306 were analyzed by an examiner blind to the experimental group (Figure 5A). Freezing
307 behavior was defined as no movements, except those resulting from breathing, that last a
308 minimum of 3 s (within each 3 s time epoch). Results were expressed as the percentage
309 of freezing during each CS trial (30 s - 10 epochs in which a freezing episode either
310 occurred or not)(Blanchard and Blanchard, 1972; Fanselow and Bolles, 1979; Curzon et
311 al., 2009). Periods outside of the CS presentation were not considered for quantification.

312

313 *LFP recordings and data analysis.*

314

315 LFP signals from the ventral region of the left IC central nucleus were recorded
316 during the CFC test sessions (Figure 7). The signals were obtained through a pre-
317 amplified unit gain stage (1x gain. ZCA-AMN16 adapter. Omnetics ©. Tucker-Davis
318 Technologies) coupled to a thin recording cable (ZC16 - 16 channel ZIF-CLIP® digital
319 head stages. Tucker-Davis Technologies). A small adapter was built into a printed circuit
320 board so that the commercial pre-amplified unit gain stage coupled to the RJ-11 connector
321 surgically implanted in the experimental animals. The signals were filtered between 1 and
322 2,000 Hz, amplified by 24,000 V/V and sampled at approximately 12 kHz by a
323 bioamplifier processor (Tucker-Davis Technologies RZ2).

324 The timestamps locked to the peaks and valleys of the CS modulating frequency
325 were generated in parallel through one of the Arduino Digital I/O pins and then recorded
326 by a digital input port of the bioamplifier processor. Through linear interpolation, these
327 time values were used to obtain an instantaneous phase time series, which in turn were
328 used to reconstruct/estimate the CS modulating signal itself. In this sense the time-
329 frequency analysis could keep engaged with the stimulus presentation.

330 The data were off-line preprocessed and analyzed with custom-made and built-in
331 MATLAB codes (MATLAB R2016a. EEG lab. *Open source environment for*
332 *electrophysiological signal processing* - <http://sccn.ucsd.edu/eeglab/>). Time-frequency
333 power of the SSEP (frequency range 40 - 70 Hz) were calculated by the standard built-in
334 spectrogram function (short-time Fourier transform-STFT; non overlapping, 16,384-
335 point Hamming window).

336 To calculate the Δ phase between CS amplitude modulating envelope and SSEP,
337 the data were initially filtered at the frequency range of 53.7 ± 3 Hz and the coefficients
338 were extracted by the built-in MATLAB function Hilbert transform. The Δ phase was
339 calculated in the average time windows of 250 ms as the difference between the imaginary
340 components of SSEP and the CS envelope:

341

342

$$\text{Mean } \Delta \text{ phase} = \frac{1}{N} \arg \left[\sum_{n=1}^N e^{i(\phi_{SSEP} - \phi_{CS})} \right]$$

343

344 Mean Δ phase: argument of the sum of the phase vectors, where N is the number of time-
345 axis samples of each signal and ϕ_{SSEP} and ϕ_{CS} are the phase values for the SSEP and
346 CS envelope, respectively.

347 The phase coherence between CS envelope and SSEP was extracted by means of
348 the length of the average vector of phase angles differences:

349

350

$$\text{Phase coherence} = \frac{1}{N} \left| \sum_{n=1}^N e^{i(\phi_{SSEP} - \phi_{CS})} \right|$$

351

352 Phase coherence: metric of phase synchronization. A dimensional real value between 0,
353 that represent an uniform phase distribution and 1, a perfect phase grouping (Lachaux et
354 al., 1999; Mormann et al., 2000) .

355

356 The dynamics of instantaneous oscillatory frequency was estimated from the
357 changes in the SSEP phase angles over time. As described above, the data was filtered
358 (range of 53.7 ± 3 Hz) and the first derivative of SSEP phase from Hilbert coefficients
359 was calculated in the average time windows of 250 ms. The phase-angle time series was
360 then transformed to a time series of instantaneous frequency by multiplying with the
361 sampling rate in hertz and then dividing by 2π (Boashash, 1992; Cohen, 2014).

361

362

$$\text{Instantaneous frequency} = \frac{fa}{2\pi} \frac{d\phi}{dt}$$

363

364 Instantaneous frequency: frequency component linearly proportional present in the
365 modulating signal. Where fa indicates the sampling rate and $d\phi/dt$ indicates
366 instantaneous variation of unwrapped angles over time.

367

368 *Statistical analysis*

369

370 The quantitative data are expressed as means \pm standard error of the mean (SEM).
371 The approximation to the normal distribution was confirmed by the Kolmogorov–
372 Smirnov test ($P > 0.05$). Statistical comparisons were made using Student's t-test or one-
373 way or two-way repeated-measures analysis of variance (ANOVA), followed by
374 Bonferroni post hoc test. For some analyses Two Sample Kolmogorov–Smirnov test was
375 used to test whether two samples come from the same distribution. Values of $P < 0.05$
376 were considered statistically significant. Data were analyzed using GraphPad Prism 7.0a
377 Software and MATLAB (2016a), The Mathworks, Natick, USA.

378

379

380

RESULTS

381

382

Bench test - CS and US stimuli.

383

384

385 The auditory stimulation system allows setting the carrier frequency in range of 1
386 Hz up to more than 100KHz. In addition, the sound stimulus can be modulated in
387 amplitude, also over a wide range of frequencies. Another flexible characteristic of the
388 auditory stimulation is its intensity, which can be programmed by controlling the
389 amplitude of the Arduino digital port output. Some carrier and modulating frequencies
390 were chosen to be depicted in Figure 4. Figure shows that the parameters were adjusted
391 accurately. The amplitude of the programmed tone (in this case 10 kHz carrier frequency)
392 remains stable at its various programmed levels (Figure 4E) and the amplitude of the
393 recorded tones (2 kHz - 20 kHz carrier frequency, Figure 4F; 50 Hz, 100 Hz, 150 Hz and
200 Hz modulating frequency, Figure 4G) remains constant over time.

394

395

396

Regarding the aversive sensory stimulus, it also exhibited precisely configurable
patterns, both temporal (number of pulses per second) and intensity (in μA) (Figure 6C).
In addition, the footshock system showed little susceptibility to changes on animal body

397 conductance. A 25 % deviation around the 20 k Ω simulated rat resistance caused, in the
398 worst case ($R = 25$ k Ω), a corresponding variation of only 4.74% (about 18 μ A) in the
399 expected shock intensity, which was 400 μ A (Figure 6F). We understand that the effect
400 of this on the experimental protocol is negligible and does not harm the behavioral data
401 obtained with the custom box.

402 It is worth noting that this slight variation in shock intensity was only possible
403 because the operating voltage of the shock circuitry is relatively high. The 310 V_{DC}
404 potential requires resistors of 300 k Ω or more to limit the shock intensity under 1000 μ A.
405 Since the animal resistance is much smaller than 300 k Ω , the shock intensity is largely
406 determined by the resistors in the electronic circuitry rather than by the animal itself.

407 It should be noted that the *Stimuli.ino* and *Control_Box.ino* sketches can be easily
408 modified to specify which bars will be used to apply footshock. This allows creating
409 different spatial patterns of aversive electrical stimulation, which in turn makes it possible
410 to perform different behavioral tasks.

411

412 *Classical fear conditioning with an amplitude modulated tone*

413

414 Over the past decade, many studies have shown that auditory fear conditioning is
415 able to induce the emergence of defensive behaviors (Maren, 2001). This traditional task
416 can be considered one of the most important methodological tools that allow
417 understanding of the underlying mechanisms of learning and memory (Collins, 2000;
418 Duvarci and Pare, 2014; Maren et al., 2001; Quirk et al., 1995).

419 In the present work the animals submitted to the CFC in the customized chamber
420 presented a robust conditioned response (Figure 5 B-C). According to the results, in the
421 preconditioning session, the auditory stimulus can be considered a neutral stimulus since
422 it did not elicit high levels of freezing. However, in the test session, 24 h after the
423 conditioning session, the paired group showed a significant increase of Freezing behavior
424 ($F_{(1,8)} = 34.26$; $p < 0.0001$), while the unpaired group maintained the baseline values as
425 the preconditioning session. The comparison between the paired and unpaired groups
426 showed significant differences in the test session ($F_{(1,8)} = 34.26$; $p < 0.0001$).

427

428 *LFP recordings during the CFC Test session*

429

430 Oscillations in the auditory pathway (Rees et al., 1986) and more specifically in
431 the IC (Lockmann et al., 2017; Pinto et al., 2017) can be entrained by the envelope of an
432 amplitude modulated tone. Furthermore, after an associative learning task in which the
433 auditory stimulus is paired with an aversive stimulus, the temporal dynamics of LFP can
434 change substantially. The phase of evoked oscillation couples to the phase of the
435 amplitude modulated tone and the power significantly increases with the auditory
436 stimulus representations (Lockmann et al., 2017). In this sense, we reproduce the data
437 previously published by our group in an attempt to prove the concept that the developed
438 chamber generates an accurate set of auditory and aversive stimuli.

439 During the CFC test session, we recorded the oscillatory activity of the ventral
440 region of the IC central nucleus in five rats from paired group. Region that, according to
441 the IC tonotopic organization, perfectly responds to high frequencies (10 kHz - CS
442 auditory stimulus). In addition, we modulate the evoked activity with a specific amplitude
443 envelope (53.7 Hz) to generate a resonant frequency, an SSEP.

444 As expected, the LFP recorded in the IC shown a distinct power spectral signature
445 embedded in the programmed fm (Figure A-B) and moreover the SSEP power during the
446 mean trials was significantly higher (~3-fold) compared to the previous instants outside

447 the trial periods (Figure 7C. $t_{(4)} = 11.42$; $p = 0.0003$).

448 The qualitative analysis of delta phase values extracted from the Hilbert
449 coefficients demonstrates that the angles are organized in clusters without major changes
450 in the mean values. In addition, the data shown a high phase coherence values over each
451 trial, suggesting a high level of synchronization between CS envelope and the SSEP
452 (Figure 7D-E).

453 Finally, the distribution of instantaneous oscillatory frequencies over trials
454 presented a variation around the modulation frequency, being significantly different from
455 the distribution instantaneous oscillatory frequencies extracted from the previous instants
456 outside the trial periods (Figure 7F-G. $KS = 0.3343$; $p < 0.0001$).

457

458

459 5. DISCUSSION

460

461 The proposed conditioning chamber has an auditory stimulation system which
462 exhibited versatility in programming stimuli characteristics (carrier frequency,
463 modulating frequency, intensity and duration). Furthermore, the equipment also has an
464 aversive stimulation system, based on footshocks applied through electrified bars.
465 Footshock intensity and duration, as well as the number of constant-current pulses per
466 second, can be properly adjusted.

467 It is important to highlight that the versatility regarding the auditory stimulation
468 system has an important application in providing a characteristic spectral signature in LFP
469 electrophysiological recordings of brain structures processing the sensory stimuli.
470 Lockmann et al (2017) has shown that a pure, continuous and amplitude-modulated tone
471 may acquire biological relevance since the neural activity of inferior colliculus,
472 responsible for one of the first stages of auditory processing, presents significant changes
473 in their temporal dynamics after conditioning. It is important to highlight that the SSEP
474 provides a unique perspective on evaluating circuitry involved in sensory signal
475 processing once its "tags" the electrophysiological recordings of such brain substrates
476 with a distinct spectral signature assigned by the modulation frequency.

477 In addition, the conditioning chamber architecture allows adding new components
478 to its design with little effort, for example: infrared sensors, touchscreens, servomotors
479 (i.e driving water and food dispensers), among others. This increases the equipment
480 usability as a tool for customized scientific protocol design.

481 As a high-level programming language platform, and with all community support
482 via forums, the Arduino IDE also enables collaborative effort to enhance and enrich the
483 chamber software routines (*Web_page.ino* and *Stimuli.ino* sketches). Our project is being
484 made available through open-source initiatives [https:// github.com/ fgmourao/
485 NNC_repository](https://github.com/fgmourao/NNC_repository)) and may be modified by collaborators adding new features to both
486 hardware and software. In this publication all the files and tutorials will be available as
487 supplementary materials.

488 The initiative to build custom equipment encourages the development of unique
489 investigation methods, exploring the peculiarities of each research group. Versatile and
490 flexible features also allow studying cognitive and behavioral processes that are not
491 observable with ordinary equipment. Finally, this custom equipment is also a low-cost
492 alternatives to commercially available devices, making them a very interesting solution
493 for cognition and behavioral research in animals.

494

495

496

497 **ACKNOWLEDGMENTS**

498

499 We would like to thank Grace Schenatto Pereira Moraes for helpful comments on
500 the manuscript and Davi Barreto Mourão e Frederico José Barreto Mourão for scientific
501 inspiration.

502

503

504 **AUTHOR CONTRIBUTIONS STATEMENT**

505

506 Projected conceived and designed by P.A.A.J., F.A.G.M. and M.F.D.M.;
507 P.A.A.J., F.A.G.M., M.C.L.A. and M.F.D.M. designed the hardware and code; P.A.A.J.,
508 performed sound and footshock validations; H.P.P., performed behavioral tests; L.O.G.,
509 performed behavioral analysis; F.A.G.M., H.P.P., performed surgery and
510 electrophysiological records; F.A.G.M. and V.R.C. performed electrophysiological
511 analysis. F.A.G.M. prepared figures; H.A.M supervised and contributed to refinements
512 of the system; P.A.A.J., F.A.G.M. draft manuscript; M.F.D.M., H.P.P. and F.A.G.M.
513 edited and revised manuscript; All authors approved the final version of manuscript.

514

515

516 **FUNDING**

517

518 This work was supported by CNPq (307354/2017-2 and 425746/2018-6), CAPES
519 (PROCAD2013-184014 and STINT 88881.155788/2017-01) and FAPEMIG (CBB -
520 APQ-03261-16).

521

522

523 **CONFLICT OF INTEREST STATEMENT**

524

525 The authors declare the absence of any personal, professional or financial
526 relationships that could potentially be construed as a conflict of interest.

527

528

529

530 **REFERENCES**

531

532 Baron, A. (1959). Functions of CS and US in fear conditioning. *J. Comp. Physiol.*
533 *Psychol.* 52, 591–593.

534 Blanchard, D.C., Blanchard, R.J. (1972). Innate and conditioned reactions to threat in rats
535 with amygdaloid lesions. *J. Comp. Physiol. Psychol.* 81, 281–290.

536 Boashash, B. (1992). Estimating and interpreting the instantaneous frequency of a signal.
537 I. Fundamentals. *Proceedings of the IEEE.* 80, 520–538.

538 Buccino, A.P., Lepperød, M.E., Dragly, S.-A., Häfliger, P., Fyhn, M., Hafting, T. (2018).
539 Open source modules for tracking animal behavior and closed-loop stimulation
540 based on Open Ephys and Bonsai. *J. Neural Eng.* 15, 055002.

541 Clopton, B.M., Winfield, J.A. (1973). Tonotopic organization in the inferior colliculus of
542 the rat. *Brain Research.* 56, 355–358.

543 Cohen, M.X. (2014). Fluctuations in oscillation frequency control spike timing and
544 coordinate neural networks. *J. Neurosci.* 34, 8988–8998.

545 Collins, D.R. (2000). Differential Fear Conditioning Induces Reciprocal Changes in the
546 Sensory Responses of Lateral Amygdala Neurons to the CS and CS-. *Learning &*

- 547 Memory. 7, 97–103.
- 548 Curzon, P., Rustay, N.R., Browman, K.E. (2009). Cued and contextual fear conditioning
549 for rodents. In: *Methods of Behavior Analysis in Neuroscience*, edited by
550 Buccafusco JJ. Boca Raton, FL: CRC.
- 551 Cushman, J.D., Aharoni, D.B., Willers, B., Ravassard, P., Kees, A., Vuong, C., Popeney,
552 B., Arisaka, K., Mehta, M.R. (2013). Multisensory control of multimodal behavior:
553 do the legs know what the tongue is doing? *PLoS One* 8, e80465.
- 554 D’Ausilio, A. (2012). Arduino: A low-cost multipurpose lab equipment. *Behavior*
555 *Research Methods*. 2, 305–313.
- 556 Davis, M., Astrachan, D.I. (1978). Conditioned fear and startle magnitude: effects of
557 different footshock or backshock intensities used in training. *J. Exp. Psychol. Anim.*
558 *Behav. Process.* 4, 95–103.
- 559 Duvarci, S., Pare, D. (2014). Amygdala microcircuits controlling learned fear. *Neuron*
560 82, 966–980.
- 561 Fanselow, M.S., Bolles, R.C. (1979). Naloxone and shock-elicited freezing in the rat. *J.*
562 *Comp. Physiol. Psychol.* 93, 736–744.
- 563 Holland, P.C. (1977). Conditioned stimulus as a determinant of the form of the Pavlovian
564 conditioned response. *J. Exp. Psychol. Anim. Behav. Process.* 3, 77–104.
- 565 Kim, J.J., Jung, M.W. (2006). Neural circuits and mechanisms involved in Pavlovian fear
566 conditioning: a critical review. *Neurosci. Biobehav. Rev.* 30, 188–202.
- 567 Kuwada, S., Batra, R., Maher, V.L. (1986). Scalp potentials of normal and hearing-
568 impaired subjects in response to sinusoidally amplitude-modulated tones. *Hear. Res.*
569 21, 179–192.
- 570 Lachaux, J.-P., Rodriguez, E., Martinerie, J., Varela, F.J. (1999). Measuring phase
571 synchrony in brain signals. *Human Brain Mapping*. 8, 194–208.
- 572 Lockmann, A.L.V., Mourão, F.A.G., Moraes, M.F.D. (2017). Auditory fear conditioning
573 modifies steady-state evoked potentials in the rat inferior colliculus. *J. Neurophysiol.*
574 118, 1012–1020.
- 575 Malmierca, M.S., Izquierdo, M.A., Cristaudo, S., Hernández, O., Pérez-González, D.,
576 Covey, E., Oliver, D.L. (2008). A discontinuous tonotopic organization in the
577 inferior colliculus of the rat. *J. Neurosci.* 28, 4767–4776.
- 578 Maren, S. (2001). Neurobiology of Pavlovian Fear Conditioning. *Annual Review of*
579 *Neuroscience*. 24, 897–931.
- 580 Maren, S., Yap, S.A., Goosens, K.A. (2001). The amygdala is essential for the
581 development of neuronal plasticity in the medial geniculate nucleus during auditory
582 fear conditioning in rats. *J. Neurosci.* 21, RC135.
- 583 Meeren, H.K.M., van Walsum, A.M. van C., van Luijckelaar, E.L.J.M., Coenen, A.M.L.
584 (2001). Auditory evoked potentials from auditory cortex, medial geniculate nucleus,
585 and inferior colliculus during sleep–wake states and spike-wave discharges in the
586 WAG/Rij rat. *Brain Research*. 898, 321–331.
- 587 Mormann, F., Lehnertz, K., David, P., Elger, C.E. (2000). Mean phase coherence as a
588 measure for phase synchronization and its application to the EEG of epilepsy
589 patients. *Physica D: Nonlinear Phenomena*. 144, 358–369.
- 590 Mourão, F.A.G., Lockmann, A.L.V., Castro, G.P., de Castro Medeiros, D., Reis, M.P.,
591 Pereira, G.S., Massensini, A.R., Moraes, M.F.D. (2016). Triggering Different Brain
592 States Using Asynchronous Serial Communication to the Rat Amygdala. *Cereb.*
593 *Cortex* 26, 1866–1877.
- 594 Picton, T.W., Sasha John, M., Purcell, D.W., Plourde, G. (2003). Human Auditory
595 Steady-State Responses: The Effects of Recording Technique and State of Arousal.
596 *Anesthesia & Analgesia*. 97, 1396–1402.

- 597 Pineño, O. (2014). ArduiPod Box: A low-cost and open-source Skinner box using an iPod
598 Touch and an Arduino microcontroller. *Behavior Research Methods*. 46, 196–205.
- 599 Pinto, H.P.P., Carvalho, V.R., Medeiros, D. de C., Almeida, A.F.S., Mendes, E.M.A.M.,
600 Moraes, M.F.D. (2017). Auditory processing assessment suggests that Wistar
601 audiogenic rat neural networks are prone to entrainment. *Neuroscience* 347, 48–56.
- 602 Quirk, G.J., Christopher Repa, J., LeDoux, J.E. (1995). Fear conditioning enhances short-
603 latency auditory responses of lateral amygdala neurons: Parallel recordings in the
604 freely behaving rat. *Neuron*. 15, 1029–1039.
- 605 Rees, A., Green, G.G., Kay, R.H. (1986). Steady-state evoked responses to sinusoidally
606 amplitude-modulated sounds recorded in man. *Hear. Res.* 23, 123–133.
- 607 Rescorla, R.A. (1967). Pavlovian conditioning and its proper control procedures. *Psychol.*
608 *Rev.* 74, 71–80.
- 609 Siegle, J.H., López, A.C., Patel, Y.A., Abramov, K., Ohayon, S., Voigts, J. (2017). Open
610 Ephys: an open-source, plugin-based platform for multichannel electrophysiology.
611 *J. Neural Eng.* 14, 045003.
- 612 Sinard, J.H., Gershkovich, P. (2012). Custom software development for use in a clinical
613 laboratory. *J. Pathol. Inform.* 3, 44.
- 614 Squire, L.R. (2009). Memory and brain systems: 1969-2009. *J. Neurosci.* 29, 12711–
615 12716.
- 616 Teikari, P., Najjar, R.P., Malkki, H., Knoblauch, K., Dumortier, D., Gronfier, C., Cooper,
617 H.M. (2012). An inexpensive Arduino-based LED stimulator system for vision
618 research. *J. Neurosci. Methods* 211, 227–236.
- 619 Walters, G., Tullis, C. (1966). Skin resistance changes in the rat during repeated
620 encounters with electric shock. *Psychonomic Science*. 5, 359-360.
- 621 White, S.R., Amarante, L.M., Kravitz, A.V., Laubach, M. (2019). The Future is Open:
622 Open-Source Tools for Behavioral Neuroscience Research. *eNeuro*. 6, 1–5.

FIGURES

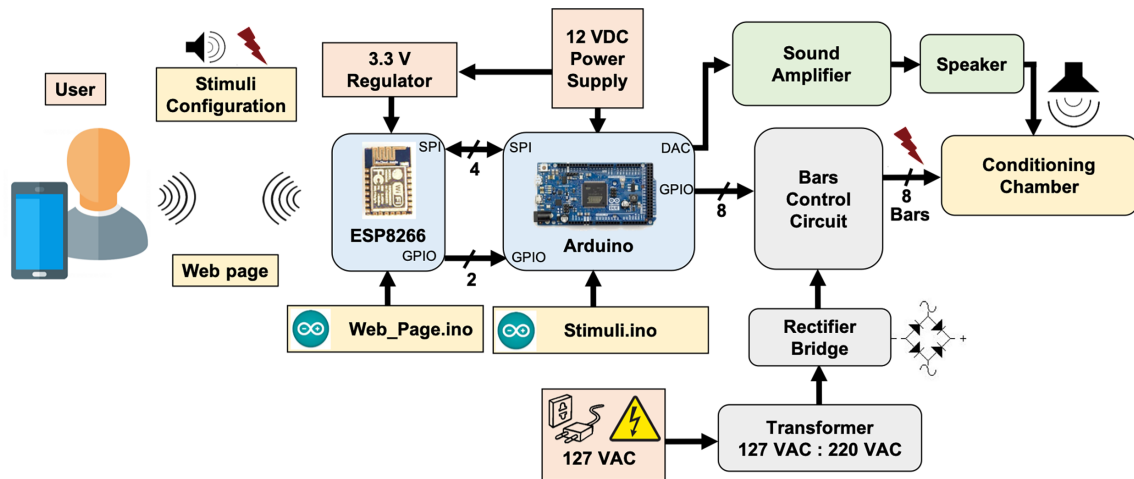


Figure 1. System overview. ESP8266-12E module and Arduino Due board cooperates in order to generate custom modulating tones and aversive stimulation, based on footshocks applied through electrified bars, programmed via user interface.

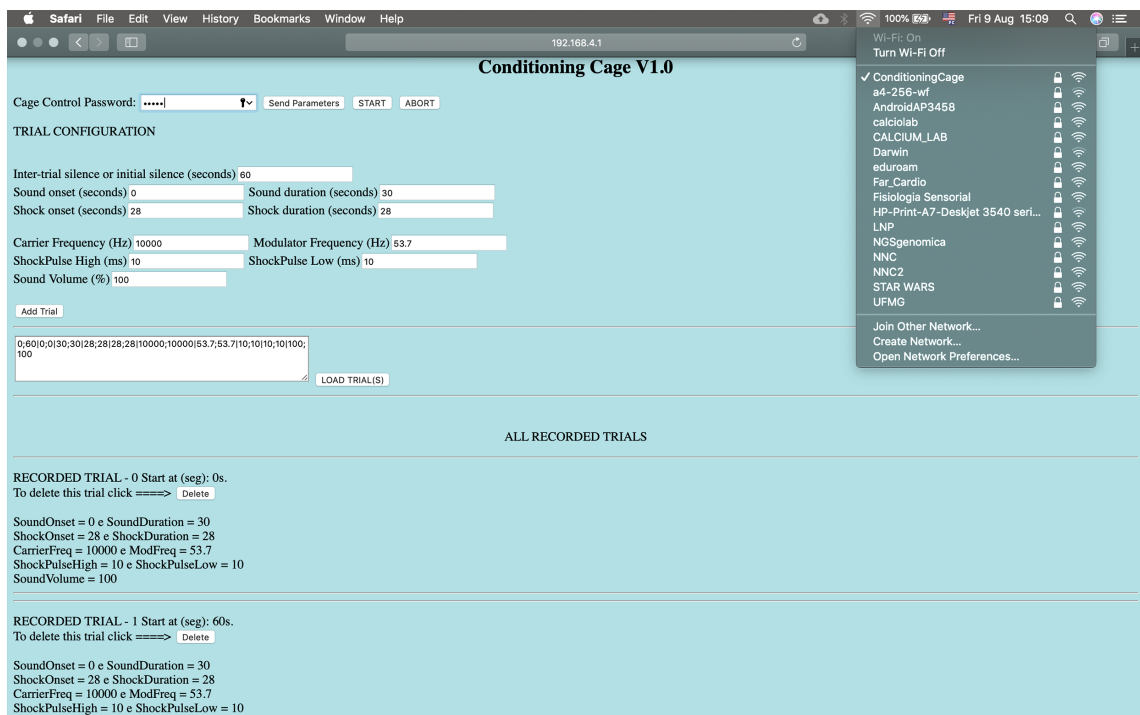


Figure 2. The conditioning chamber can be remotely controlled by a HTML interface. Parameters: Sound and shock onset (seconds), shock pulses intervals between bars (milliseconds to seconds), sound intensity (%), sound carrier frequency and modulating frequency. Each added trial can be saved by simply insert the parameters into a sequence and loaded it in later experimental sessions. Wi-Fi connection: ConditioningCage, IP address: <http://192.168.4.1>, Password: 0112358132, Cage control password to send the parameters: 12345. Start / Abort: Start and stop experiment.

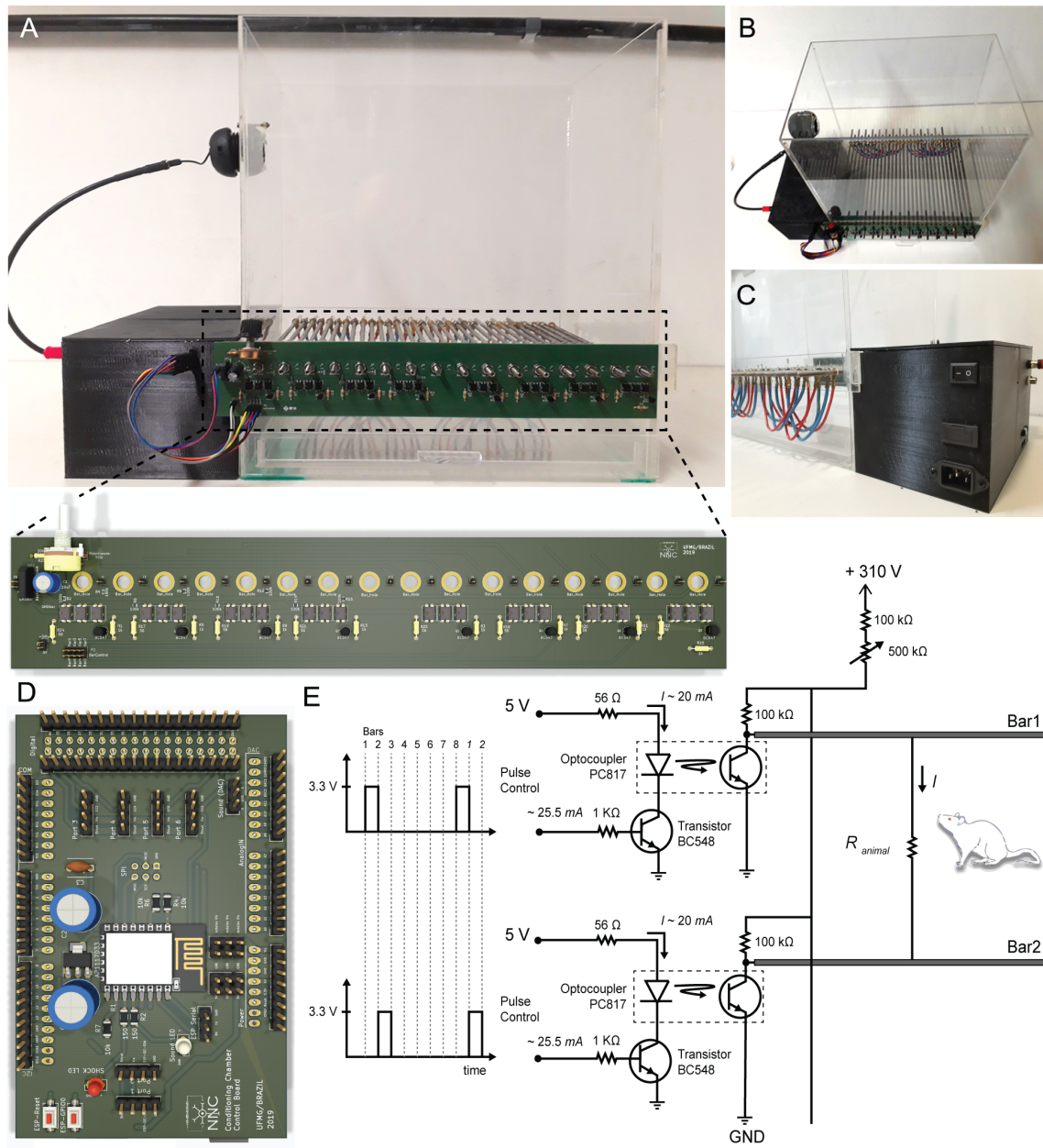


Figure 3. Hardware Design. A, *Top*) Conditioning chamber front view. *Bottom*) Two-layer printed circuit board with power circuit. Attached to the chamber via 16 mounting holes, this board allows creating electric potential between the conductive bars. B and C) Up view and back view of the conditioning chamber respectively. Detail for black box built on the 3d printer where all electronic components are organized. D) Two-layer printed circuit board with control circuit. It has ESP8266-12E footprint, Arduino Due shield and it outputs a low power audio waveform and digital signals with temporal patterns for electric stimulus control. E) Electric potential on each bar is controlled through a switch (npn transistor operating in saturation mode). A set of optocouplers are used in order to isolate power circuit from control circuit. Output voltage is 0 V_{DC} or 310 V_{DC}. Output current ranges from ~200 μ A to ~1500 μ A.

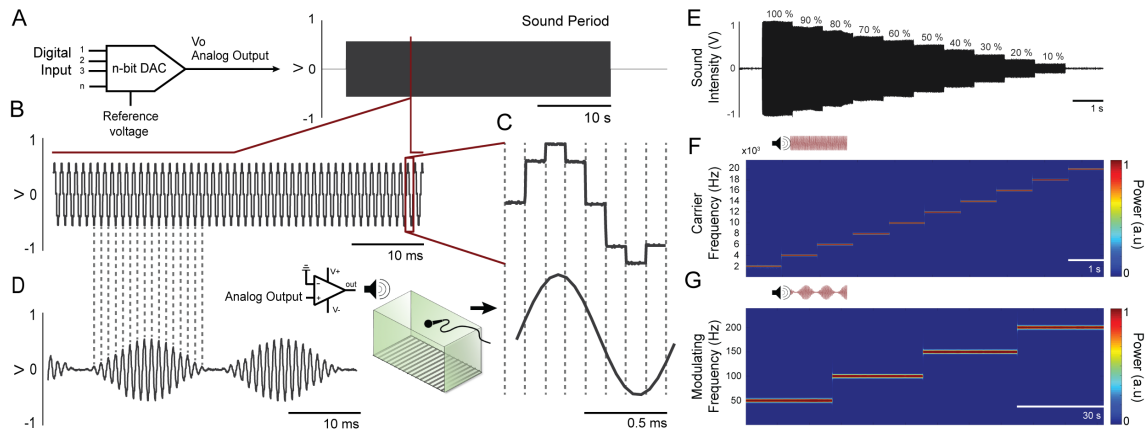


Figure 4. Waveforms can be generated from digital-to-analog converter at Arduino Due. A) A 12-bit digital-to-analog converter (DAC) is used to generate custom audio waveforms. B) Tones with adjustable frequency can be produced with 8 voltage steps within each tone cycle. Although these voltage steps introduce undesirable high frequency components on audio signal, these components can be attenuated at power amplifier circuitry, since its frequency response is similar to a low-pass filter. C) Upper waveform shows a single cycle generated at the DAC output, where the 8 voltage steps are visible. Lower waveform shows the same cycle measured at power amplifier output, which low-pass filter the audio signal and outputs a smooth waveform, practically a pure tone. D) Amplitude modulation can be applied to the audio waveform, with adjustable modulating frequency. E) The amplitude of the programmed tone It can be set to various levels. F) Time-frequency power of the carrier frequency in a range of 2 kHz - 20 kHz (steps by 2 kHz) were calculated by the short-time Fourier transform-STFT demonstrating a constant amplitude over time. G) Time-frequency power of the modulating frequency envelope in a range of 50 Hz - 200 Hz (steps by 50 Hz) were calculated by the short-time Fourier transform-STFT demonstrating a constant amplitude over time.

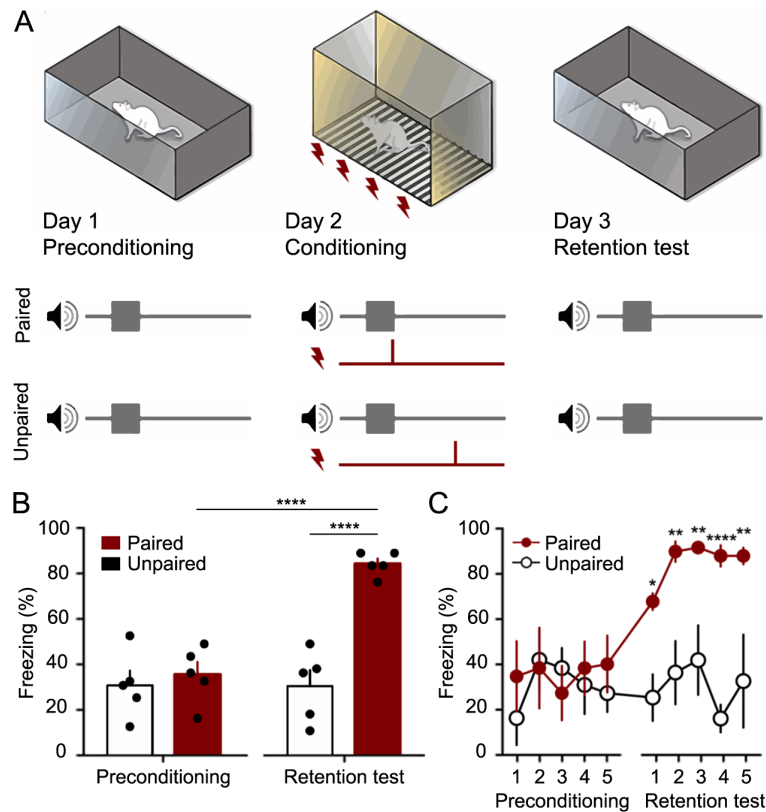


Figure 5. The Fear conditioning protocol (CFC) was performed as a proof of concept for the customized chamber. A) Preconditioning occurred in Day 1, when 5 trials of CS (10 kHz pure tone with its amplitude modulated by a sine wave of 53.7 Hz) were presented to the animals in a context A. The Conditioning occurred in Day 2, when 5 trials of CS and US (a footshock with 400 μ A over 2 s) were presented to the Paired and Unpaired groups using the customized chamber. In Day 3, retention test occurred with 5 trials of CS being presented to both groups. Animal fear response (freezing) was measured in order to verify if the association between sound and shock. B) Total mean freezing (\pm SEM) to CS in preconditioning and test sessions. C) mean freezing (\pm SEM) to CS over trials. * $p < 0.05$, ** $p < 0.01$, **** $p < 0.0001$. 2-way ANOVA followed by Bonferroni post hoc test.

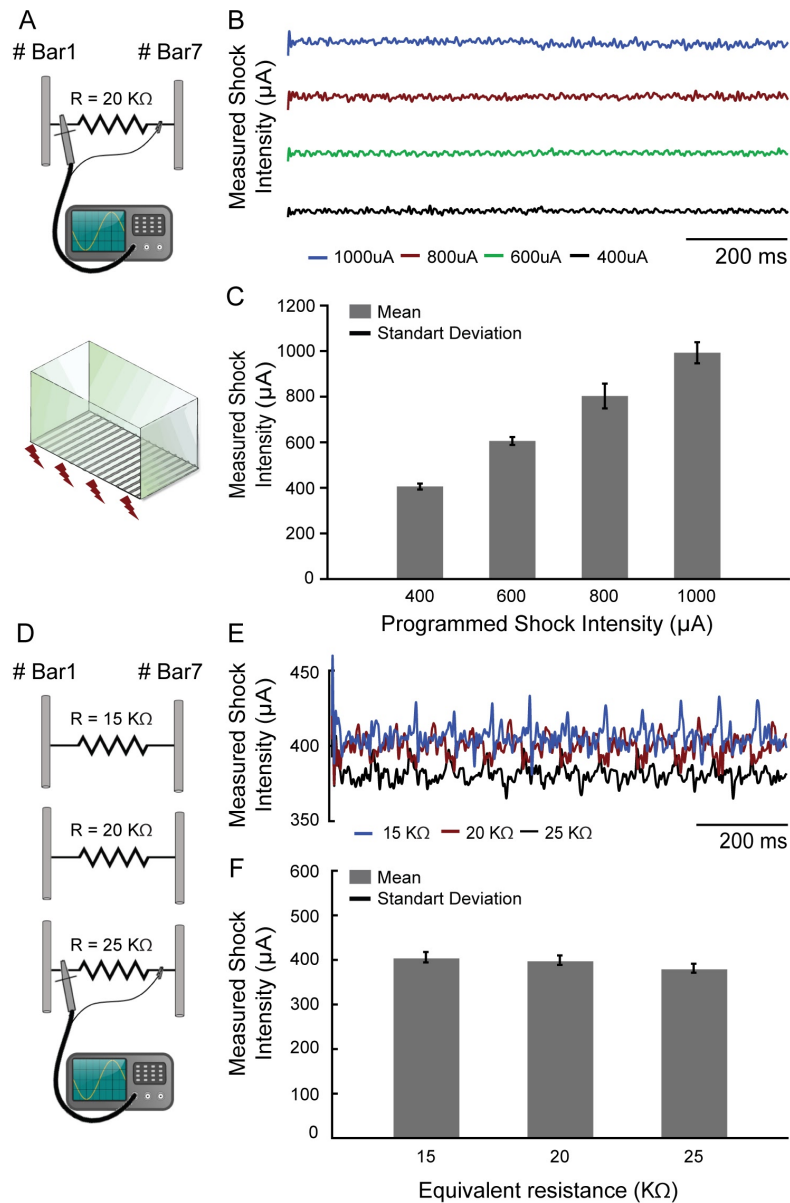


Figure 6. The footshock exhibited precisely configurable patterns. A) The footshock intensity was measured by an oscilloscope ($I = V/R$) through a resistor that simulates the animal skin resistance. B) The current measurements were made over time in four different programmed shock intensities (μA). C) The mean footshock intensities remaining constant and showed no significant changes. D) The same measurement was performed with three different resistors at a programmed current value to simulate the skin resistance variations. E) The current measurements were made in one programmed value (400 μA) over time. F) The values with a 25 % deviation around the 20 $\text{k}\Omega$ caused no significant changes in the programmed shock intensities. (maximum $\sim 4.74\%$, $\sim 18\ \mu\text{A}$, to 25 $\text{k}\Omega$).

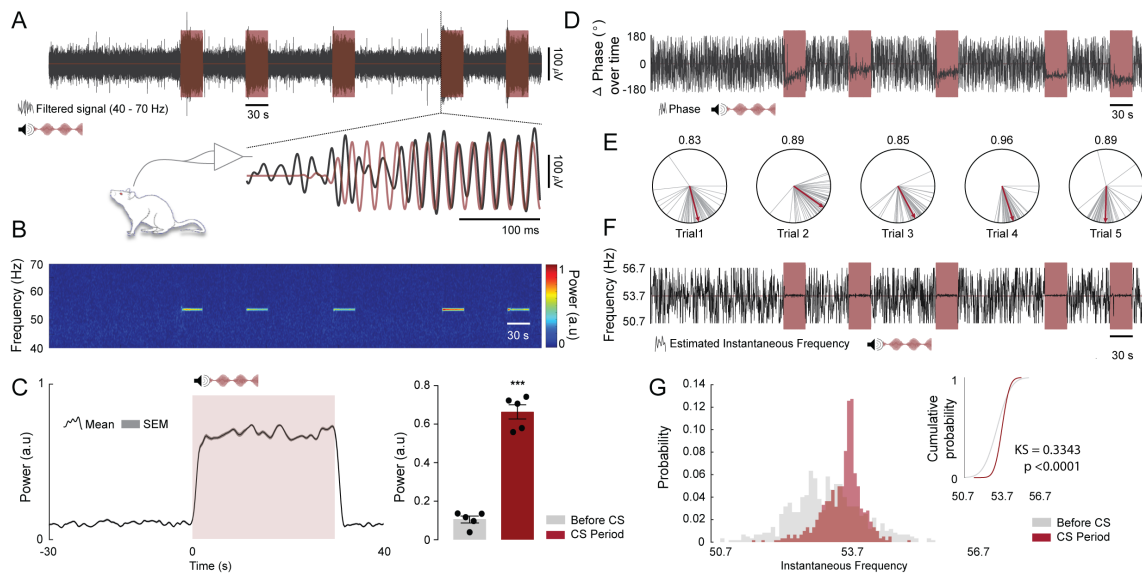


Figure 7. Oscillations in the IC can be entrained by the envelope of an amplitude modulated tone. A, top) Representative time course of LFP (grey) and CS trials (light red, 10 kHz pure tone with an amplitude modulation of 53.7 Hz). A, Bottom) Highlight to a sample time window at the beginning of the fourth trial showing that the IC LFP synchronizes with the CS amplitude envelope. The LFP and the CS envelope were band-pass filtered between 40 and 70 Hz. B) Spectrogram showing SSEP power at 53.7 Hz (a.u., Arbitrary units). C, left) Mean SSEP power at 53.7 Hz ± 3 Hz over trials for all animals. The figure shows a period of 30 seconds before CS onset, 30 seconds of CS presentation and 10 seconds after. C, right) Qualitative analysis of SSEP power at 53.7 Hz ± 3 Hz for 30 seconds before CS onset compared to the 30 seconds of CS presentation (n = 5 animals; before CS vs. CS period; $t_{(4)} = 11.42$, $p = 0.0003$). D) Representative time course of delta phase values at 53.7 Hz ± 3 Hz ($\phi_{SSEP} - \phi_{CS}$) extracted from the Hilbert coefficients (grey) and CS trials (light red). E) Delta phase vectors computed for 250 ms time windows during CS presentation (grey lines) and the respective estimate mean phase values (red lines). The numbers above the polar plots represents the phase coherence of each trial during CS presentation. F) Representative time course of instantaneous oscillatory frequency estimated at 53.7 Hz ± 3 Hz from the changes in the SSEP phase angles (grey) and CS trials (light red). G) Distribution of instantaneous oscillatory frequencies over trials for 30 seconds before CS onset (light grey) and 30 seconds of CS presentation (light red) and their respective cumulative distributions. Two Sample Kolmogorov–Smirnov test was used to test whether the two samples come from the same distribution (n = 5 animals; before CS vs. CS period delta phase angles distributions; $KS = 0.3343$, $p < 0.0001$).